SUPPLEMENTAL MATERIAL

Supplemental methods

Structure determination was hindered by the presence of pseudo translational symmetry, which masked merohedral twinning. Initially, crystals of W174R mutant (W174R-acidic) were indexed in space group P321 with a=b=117.08 Å, c= 321.37 Å, α=β=90°, γ=120°. Inspection of the native Patterson maps, calculated in CCP4 (S2), showed a large peak at U,V,W=0, 0, 0.5 suggesting the presence of pseudo translational symmetry. This would be consistent with two gB protomers in the asymmetric unit arranged top-to-bottom along the crystal c axis. Analysis using *phenix.xtriage* confirmed the correct assignment of the space group and the presence of pseudo translational symmetry, with an off-origin peak of ~75% of the origin peak. At this point, twinning was not detected by any of the several software programs used, including *phenix.xtriage* (S1) and the UCLA twinning server (S6). Analysis using *phenix.xtriage* reported no suspected twinning, but found a twin law (-h, -k, l) with a twin fraction of 0.022 while the UCLA twinning server reported the twin fraction to be 0.0057.

The W174R-acidic structure was solved using molecular replacement (MR) with Phaser (S5) and chain A of trypsin-cleaved wt-gB-neutral structure (S3) (pdb accession code 2GUM) as a search model. MR search located two protomers of gB belonging to two different trimers generated by threefold crystallographic symmetry. The MR solution was used as a starting model for refinement in *phenix.refine* (S1) using data from 47.3 to 2.26 Å resolution. However, refinement did not progress well as both R and R_{free} remained high. Moreover, inclusion of TLS in refinement, while lowering the R and R_{free}, resulted in streaky maps that appeared to be of lower resolution. These observations suggested that the initial space group assignment, P321, was incorrect and that the real space group had a lower symmetry.

Next, the data were reprocessed in P3 space group. Although *phenix.xtriage* kept suggesting that P321 was the correct space group, it now also detected merohedral twinning with the twin law (h, -h-k, -l) and the twin fraction of 0.478. The UCLA twinning server also detected merohedral twinning with the same twin law but a somewhat lower twin fraction, 0.405. As in P321, pseudo translational symmetry was detected in a native Patterson map, with an off-origin peak of ~75% of the origin peak. Presence of pseudo translational symmetry is known to confound the detection of twinning (S7) and likely happened here.

MR search in P3 located four protomers of gB belonging to four different trimers generated by threefold crystallographic symmetry. Subsequent refinement resulted in excellent maps and good-quality statistics. All data were then reprocessed in P3 space group.

Table S1: Missing Residues

Molecule	Chain	N-terminus	Domain I	Domain II	C-Terminus
wt-gB-neutral[a]	A	28-110	331-337	460-491	726-730
wt-gB-neutral[a]	B	28-108	331-336	462-490	725-730
wt-gB-neutral[a]	C	28-108	328-336	460-490	724-730
W174R-acidic	A	28-102		478-491	725-730
W174R-acidic	B	28-102		477-491	725-730
W174R-acidic	C	28-102		478-491	725-730
W174R-acidic	D	28-102		478-491	725-730
Y179S-acidic	A	28-103		478-491	724-730
Y179S-acidic	B	28-104	261-263	476-490	726-730
Y179S-acidic	C	28-103		476-491	724-730
Y179S-acidic	D	28-103	261-263	478-491	726-730
Y179S-basic	A	28-102		477-491	725-730
Y179S-basic	B	28-102		476-491	725-730
Y179S-basic	C	28-103		476-491	725-730
Y179S-basic	D	28-102		479-491	725-730
wt-gB-acidic	A	28-102	261-262	477-491	725-730
wt-gB-acidic	B	28-110	260-262	477-491	725-730
wt-gB-acidic	C	28-101	261-264	476-491	725-730
wt-gB-acidic	D	28-102	260-262	478-491	724-730

[a]wt-gB-neutral is 2GUM (S3)

Table S2: Representative r.m.s.d. values[a]

Structure[b]	r.m.s.d. (Cα)[c]
wt-gB-neutral chain B	0.53 Å
wt-gB-neutral chain C	0.8 Å
W174R-acidic chain A	1.19 Å
W174R-acidic chain B	0.9 Å
Y179S-acidic chain A	1.25 Å
Y179S-acidic chain B	0.74 Å
Y179S-basic chain B	0.71 Å
Y179S-basic chain C	0.77 Å
wt-gB-acidic chain A	1.14 Å
wt-gB-acidic chain B	0.68 Å

[a]calculated using SuperPose (S4).

[b]wt-gB-neutral chain was used as the reference structure.

[c]Over all shared residues, including FL2.

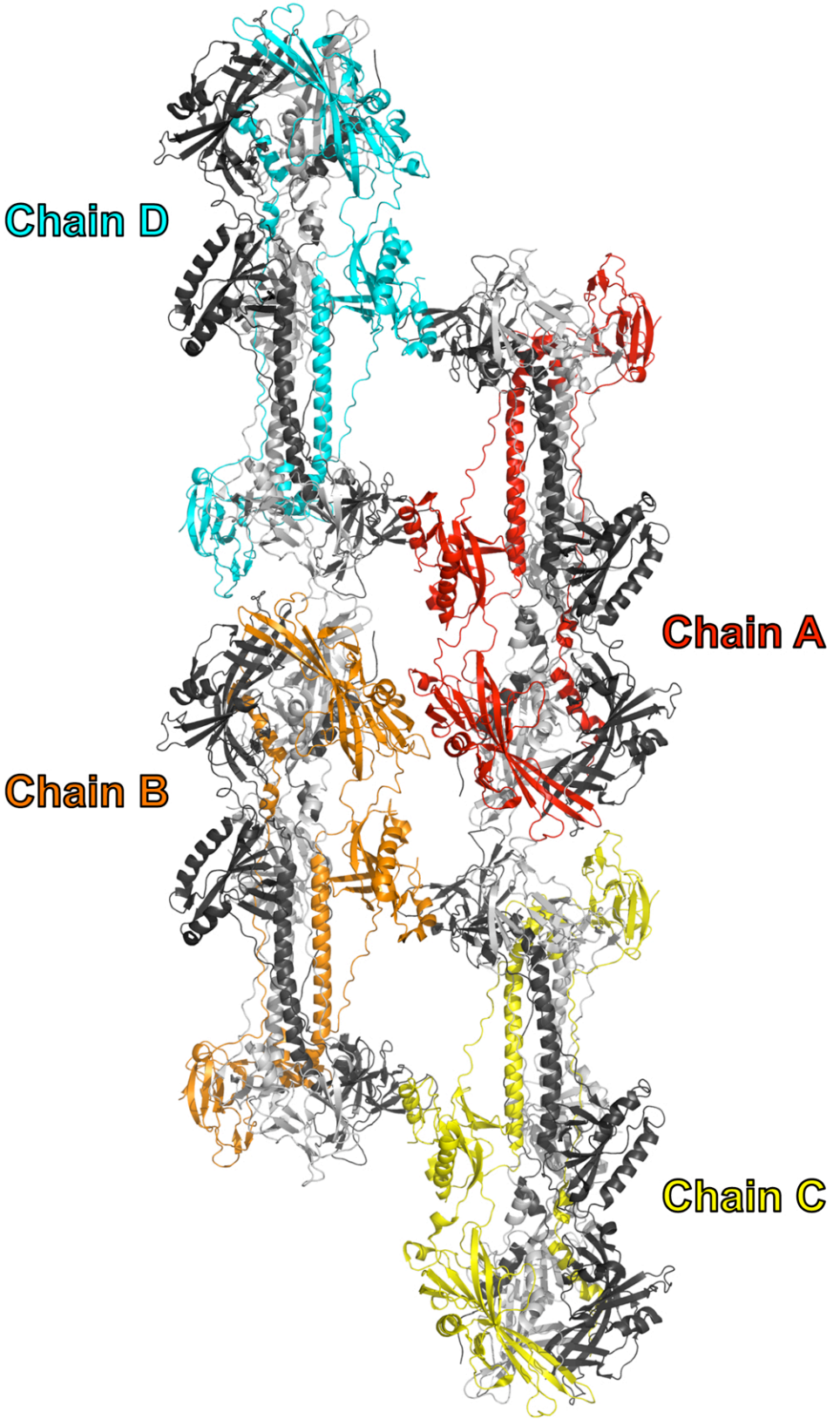

Fig. S1. 4 unique protomers within an asymmetric unit in the W174R-acidic crystals are labeled as chains A, B, C, and D and shown as red, orange, yellow, or cyan ribbons, respectively. For each unique protomer, a corresponding trimer was generated using a threefold crystallographic symmetry operation, and two other protomers in each trimer are shown in light gray and dark gray. The same arrangement is observed in the structures of Y179S-acidic, Y179S-basic, and wt-gB-acidic (not shown).

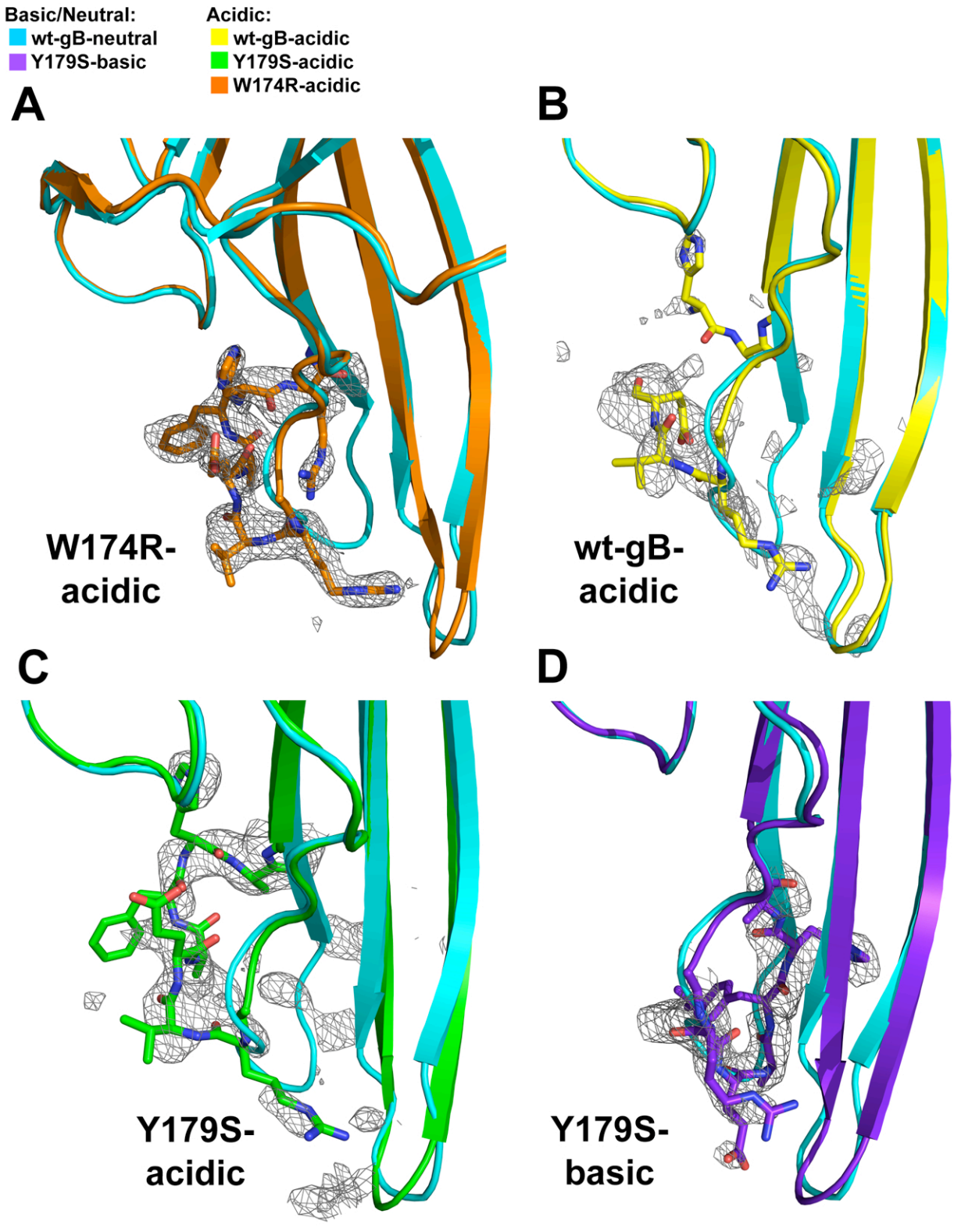

Fig. S2. Electron-density omit maps (FOFC) of FL2. Chain A wt-gB-neutral, in cyan, was superimposed onto all structures using residues 185-250 as a reference. The omit maps from the reference structures are shown for W174R-acidic chain B (A), wt-gB-acidic chain A (B), Y179S-acidic chain A (C), and Y179S-basic chain C (D). Electron density within a 3-Å radius (A-C) or 2-Å radius (D) of all atoms from residues 258-264 of both the reference structure and wt-gB-neutral is shown. The sigma level cutoff for the FOFC density in each panel was 3.0 (A), 2.5 (B), 2.2 (C), and 2.7 (D). Residues 258-264 are shown as sticks while the rest of the polypeptide chain is shown as a Cα ribbon. Views in A-D are shown in similar but not identical orientations.

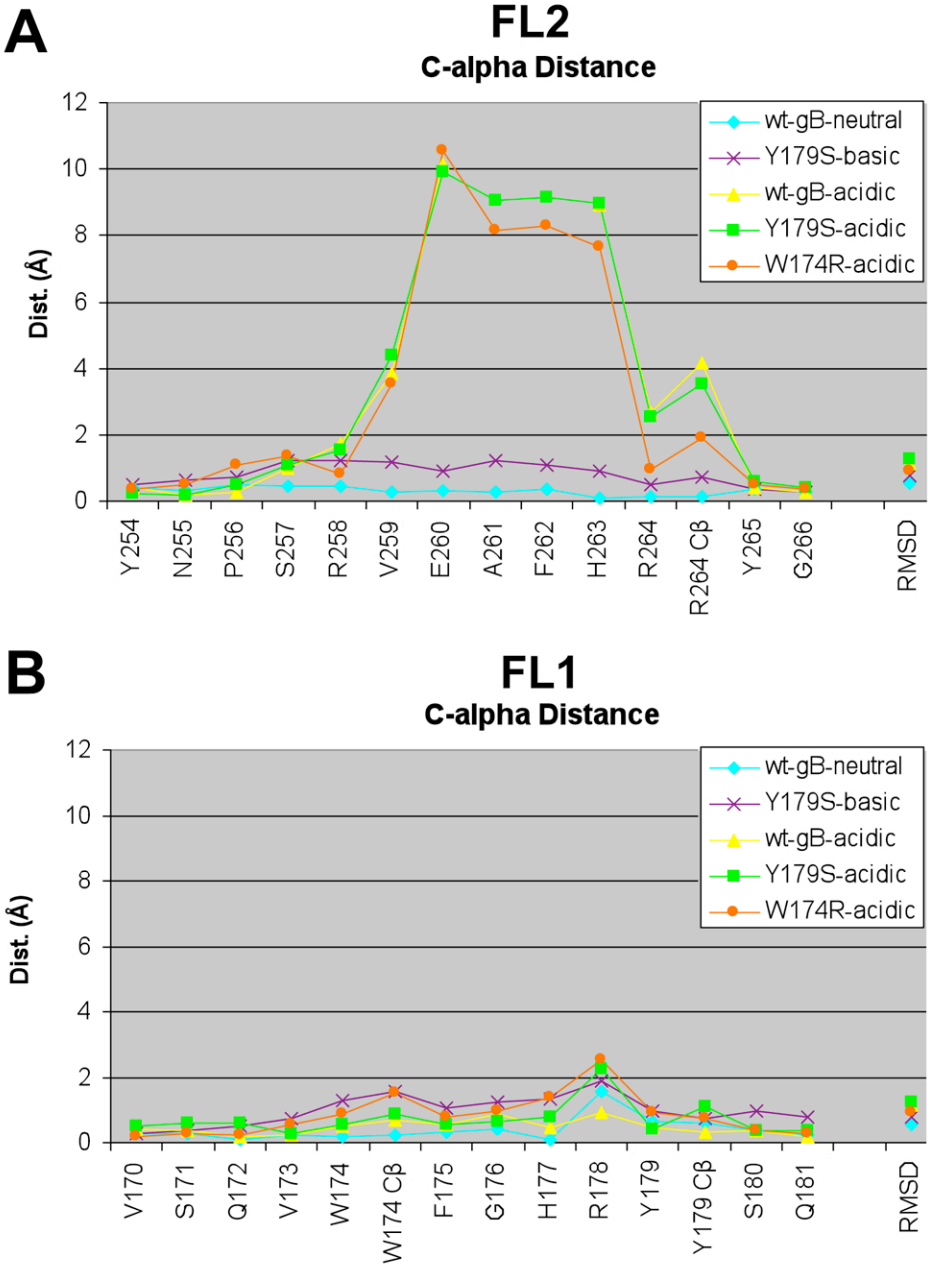

Fig. S3. FL2 (A) but not FL1 (B) undergoes conformational changes under acidic conditions. Pairwise Cα-atom (default) or Cβ-atom distances between each of the 4 structures determined here and the wt-gB-neutral structure, chain A, are plotted as a function of residue number. As a control, pairwise distances between chains B and A of the wt-gB-neutral structure are also shown. In the last column, the root mean squared deviation (R.M.S.D) for all Cα atoms within a protomer was calculated.

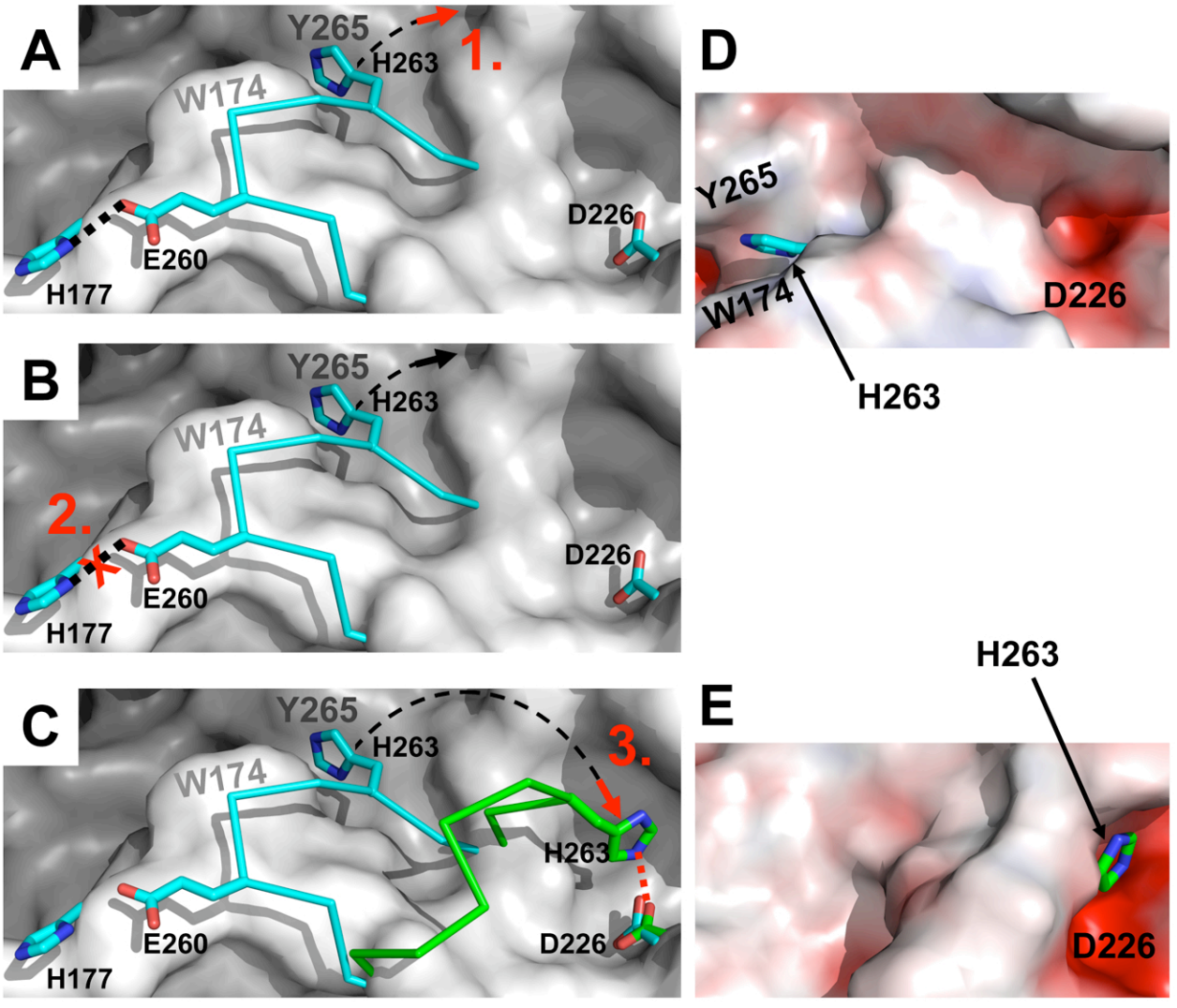

Fig. S4. Hypothetical sequence of events during the low-pH induced conformational changes in FL2. (A-C) The wt-gB-neutral structure is shown as a white surface, with residues 258-264 and the nitrogen of Y265 omitted. FL2 residues 258-264 in wt-gB-neutral (cyan) and Y179S-acidic (green) are shown as a Cα trace with key residues shown as sticks. Views in panels A-C are shown in the same orientation. (A) In step 1, H263 becomes positively charged and leaves the uncharged region between W174 and Y265. (B) In step 2, this movement pulls FL2 into solution, breaking the hydrogen bond (black dotted line) between E260 and H177, which stabilizes the neutral/inward conformation of FL2. (C) In step 3, positively-charged H263 forms a salt bridge (red dotted line) with negatively-charged D226, locking FL2 in the acidic/outward conformation. For panels A-C, a single protomer of Y179S-acidic was superimposed onto chain A of wt-gB-neutral using residues 185-250 as reference. (D, E) Electrostatic surface potential of the wt-gB-neutral (D) and Y179S-acidic (E) structures, with negative charge shown in red, and positive in blue. Electrostatic surface potential is shown on the same scale in (D) and (E). The side chains of residues F262 and H263 were omitted. H263 side chains are shown as sticks in both panels. Locations of residues D226 (D, E), W174 (D) and Y265 (D) are indicated. Views in panels D and E are shown in the same orientation.

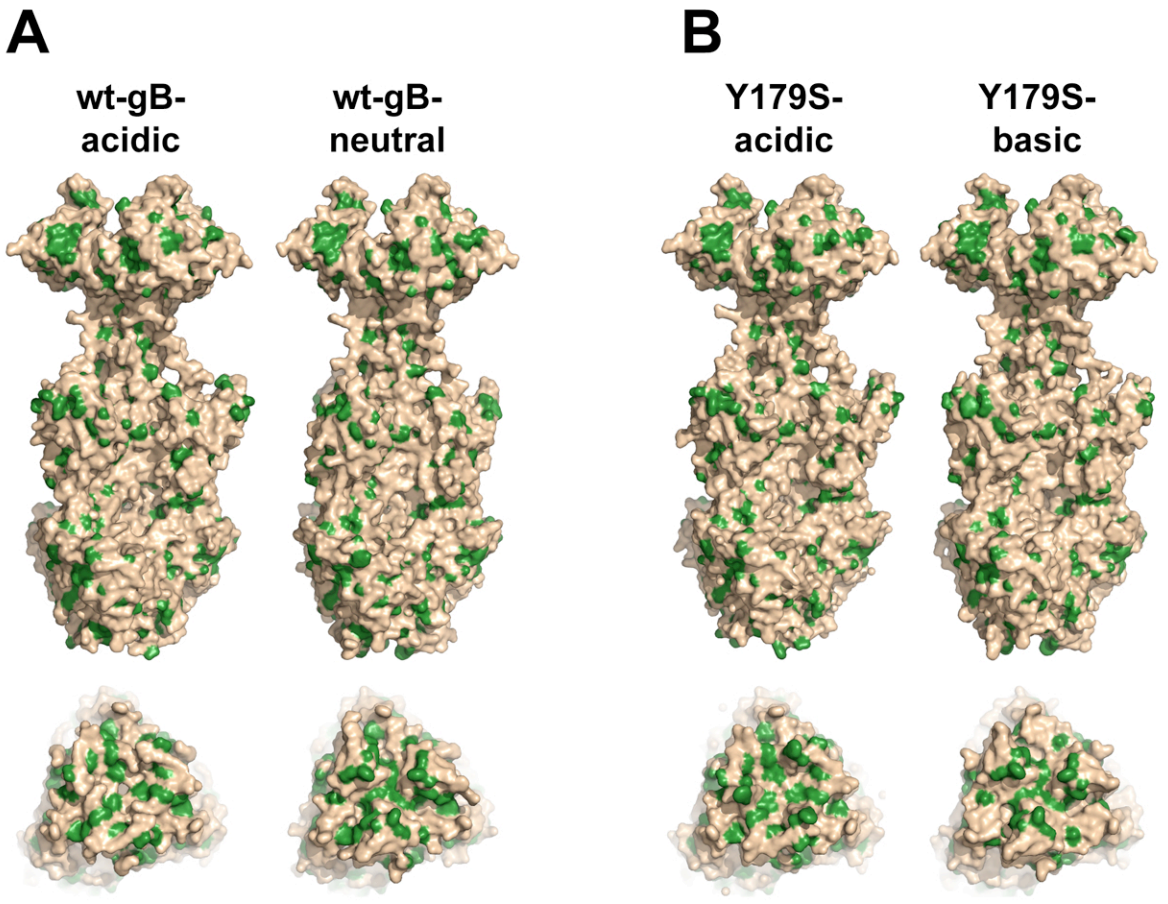

Fig. S5. Comparison of surface hydrophobicity in acidic and neutral/basic structures. Each structure is shown as a beige surface, with hydrophobic side chains (A, V, L, I, F, M, W, and Y) in green. (A) The wt-gB-acidic and wt-gB-neutral structures. (B) The Y179S-acidic and Y179S-basic structures. Top panels show the side view of the whole structure, and bottom panels show the fusion loop regions at the base of each molecule. Views in the bottom panels were generated by a 90° rotation around the horizontal axis, with the base of gB moving towards the viewer.

Supplemental references

S1. **Adams, P. D., R. W. Grosse-Kunstleve, L. W. Hung, T. R. Ioerger, A. J. McCoy, N. W. Moriarty, R. J. Read, J. C. Sacchettini, N. K. Sauter, and T. C. Terwilliger.** 2002. PHENIX: building new software for automated crystallographic structure determination. Acta Crystallogr D Biol Crystallogr **58:**1948-54.

S2. **CCP4.** 1994. The CCP4 suite: programs for protein crystallography. Acta Crystallogr D Biol Crystallogr **50:**760-3.

S3. **Heldwein, E. E., H. Lou, F. C. Bender, G. H. Cohen, R. J. Eisenberg, and S. C. Harrison.** 2006. Crystal structure of glycoprotein B from herpes simplex virus 1. Science **313:**217-220.

S4. **Maiti, R., G. H. Van Domselaar, H. Zhang, and D. S. Wishart.** 2004. SuperPose: a simple server for sophisticated structural superposition. Nucleic Acids Res **32:**W590-4.

S5. **McCoy, A. J., R. W. Grosse-Kunstleve, P. D. Adams, M. D. Winn, L. C. Storoni, and R. J. Read.** 2007. Phaser crystallographic software. J Appl Crystallogr **40:**658-674.

S6. **Padilla, J. E., and T. O. Yeates.** 2003. A statistic for local intensity differences: robustness to anisotropy and pseudo-centering and utility for detecting twinning. Acta Crystallogr D Biol Crystallogr **59:**1124-30.

S7. **Zwart, P. H., R. W. Grosse-Kunstleve, A. A. Lebedev, G. N. Murshudov, and P. D. Adams.** 2008. Surprises and pitfalls arising from (pseudo)symmetry. Acta Crystallogr D Biol Crystallogr **64:**99-107.